Original Research Article

H_{α} AND H_{β} PROFILE VARIATIONS IN THE SPECTRA OF EARLY SUPERGIANTS HD198478 AND HD187982

ABSTRACT – Profile variations in the H_{α} and H_{β} lines in the spectra of the stars HD198478 and HD187982 are investigated from observations acquired in 2010-2011, 2013-2015 at the Cassegrain focus of the 2-m telescope at the Shamakhy Astrophysical Observatory. The spectral resolution is approximately 15000.

The emission and absorption components of the H_{α} profile are found to disappear on some observational days in the spectra of HD198478. It is suggested that the observational evidence for the non-stationary atmosphere of HD198478 can be associated in part with non-spherical stellar wind.

It has been revealed that absorption in the line of H_{α} has variable structure in the spectrum of the star HD187982 depending on the activity phase of the atmosphere. The profile of the line has normal P Cyg type in the active phase of the star atmosphere. The emission component in the red wing of the profile forms and disappears. It is supposed that such variations may be due to non-stationary and strong flow substance in the atmosphere of this star.

Key words: Supergiant stars, the profile of the H_{α} line, HD198478, HD187982

I. INTRODUCTION

The study of supergiants, the most luminous stars, is of great interest in terms of the stellar and chemical evolution of galaxies. Almost all of the early supergiants are observed to show spectral and photometric variability. Due to the variable stellar wind and mass-loss rate, the spectra of the supergiants exhibit variations in the intensity, radial velocities, and P Cyg profiles of the lines of hydrogen, helium, and ions with a high degree of ionization.

In adition, a significant mass-loss rate is typical of the highest luminosity stars. In the optical region of the spectra, a particularly sensitive indicator of the rate of outflow of matter is the emission line H_{α}. The H_{α} line in the spectra of these supergiants has a clear P Cyg type profile.

The objects of these studies, the stars HD198478 (B4Ia) and HD187982 (A2Ia), are the supergiants with the following parameters, respectively [1-7]:

m_v=4.86, m_v=5.58, T_{eff}=17500K, T_{eff}=(9300±250)K, $M/M_{\odot}$=34±4, $M_*/M_{\odot}$=15, $R_*/R_{\odot}$=49, $R_*/R_{\odot}$=78, logg= 2.10, logg=1.60±0.15, vsini =61 km/s, vsini = (15±6) km/s.

The supergiant HD198478 belongs to the CygOB7 associations [8]. By analyzing spectroscopic observations of the star of HD198478, Underhill discovered large-scale irregular motions in its atmosphere [9]. By exploring the spectra obtained in 1937-1959, she found evidence of the rapid variability of the H_{α} profiles in the spectrum of this star.

On the basis of spectroscopic observations for 15 consecutive nights, Granes reported a variable pattern of the H_{α} profile [10]. The time curves of the radial velocities of the hydrogen lines gave evidence of repetitive motions of the atmosphere inside the stellar envelope. The author came to the conclusion that, apart from the 15-day variability cycles, the stellar atmosphere exhibits repetitive 4 to 5-day periodic changes.

The supergiant HD187982 belongs to the VulOB4 associations [4-5]. In the study of H_{α}, H_{γ}, MgII (4481 Å), and FeII (4924 Å, 5018 Å, 5169 Å) lines observed in the atmospheres of this supergiant is presented [4-5, 11, 12]. It is noted that generally the profiles of the H_{α} line are observed in absorption. Sometimes in the red wing of the profile of H_{α} line is observed weak emission component. A more complete explanation of appearance and disappearance of these components require additional observations.

We note that the main characteristic feature of the stars HD198478 and HD187982 are the significant variability of the spectra. The main purpose of this paper is to study the observed components of the H_α and H_β profiles in the spectra of these stars.

We believe our results will be of interest for further studies of these remarkable stars.

II. OBSERVATIONS AND PROCESSING

Spectral observations of the supergiants HD198478 and HD187982 in 2010-2011 and 2013-2015 were carried out using a CCD detector in the echelle spectrometer mounted at the Cassegrain focus of the 2-m telescope of the Shamakhy Astrophysical Observatory [13]. The spectral resolution was R=15000 and the spectral range is λλ4700-6700 Å.

Two to three spectra of the target stars were obtained on each night. The signal-to-noise ratio was S/N=150-200. The average exposure was 600-900 s, depending on the weather conditions.

In addition to the observations of the target stars, in order to check the stability of the instrument we also obtained numerous spectra of standard stars, the day and night background, and comparison spectra. The Echelle spectra were processed with the standard technique using the DECH20 and DECH20t software [14]. The reduction of the spectra, which included the continuum placement, the construction of dispersion curves (from the spectra of a hollow-cathode Th+Ar lamp or radial velocity standard stars), spectrophotometric and position measurements was performed using this package.

The measurement error for the equivalent widths W_λ was about 5%, and for the radial velocity V_r was ±2 km/s. Appropriate heliocentric corrections were included during data processing.

First, we present preliminary results of a long-term spectroscopic monitoring of a sample of bright B supergiants. Dramatic line-profile variations operating on a daily (and in some cases on a hourly) timescale are observed.

HD198478. According to the numerous spectroscopic observations, the spectra of this star display the most variable H_α line intensities and profiles. Thus, the following H_α profile variations are observed [9-10,15]:

a) H_α is in pure absorption,
b) H_α exhibits a normal P Cyg profile,
c) H_α is in pure emission,
d) H_α exhibits an inverse P Cyg profile and
e) H_α exhibiting a three-component shape: the emission profiles on both sides of central absorption component, or vise versa, the absorption profiles on both sides of central emission component.

We spectroscopically monitored HD198478 between 2010-2011 and 2013-2015. We obtained a total of 204 spectra, distributed over 102 nights.

We present the fragments of the resulting spectra covering the H_α region (Fig.1). It is revealed that in the spectra of June 27-30, 2010, the H_α line has an ordinary P Cyg-type profile, but the radial velocities (V_r) and the equivalent widths (W_λ) of H_α in emission and absorption and the lines of other elements change over time [16]. The emission component of the H_α profile shows the greatest variations, which indicates changes in the physical conditions inside the expanding stellar envelope.

But more interesting spectra were obtained on July 2-4, 2010 [16]. They appear to have no H_α line, with no spectral components apart from weak atmospheric lines and noises being observed at its wavelength (λ=6562.816 Å). At the same time, in the vicinity of the H_α line at λλ6400-6600 Å, there are two visible carbon lines CII (λ6578.05 Å, λ6582.88 Å) and weak stellar and atmospheric lines (λ6542.31 Å, 6543.91 Å, 6552.63 Å, 6557.17Å, 6558.15Å, 6561.11Å, 6564.20Å, etc.).

Interestingly, in these same spectra, all other lines typical for hot supergiants such as HD198478, apart from H_α, are observed, including H_β.

On July 5 and 6, 2010, the emission component increases, completely outshining the absorption component. Therefore, the H_α profiles of these dates display no absorption component. A similar pattern was observed later, on July 8-9, 2010. And on July 18, 2010, the H_α line was observed an ordinary normal P Cyg-type profile again.

Next observations of this star were carried out in 2011, 2013, 2014 and 2015.

Note that on July 07, 13, 2011, and on August 17, 2011, the intensities of absorption and emission components of the H_α line became weaker (r_v~ 0.96 and r_v ~ 1.04).

In 2013 and 2015 all shapes of the H_α profile in the spectra of the star HD198478 were observed classical P-Cyg-profile.

But on September 07, 2014, the profile of the H_α line is absent from the spectrum again. Further, on September 08-11, 2014, vice versa, first the absorption component became stronger unlike than in 2010. Some nights later we already observed the emission component of the H_α line (Fig.1a).

An attempt to explain the disappearance of the H_α profile in the spectra obtained before and after July 2-4, 2010, and September 07, 2014, was made by processing the lines of H_β and other elements. Table 1 presents some measurements in the H_α and H_β lines in the spectra of HD198478 star obtained in 2010 and 2014. We have determined that when the components of H_α line were observed the radial velocity and the equivalent width of the absorption and emission of H_α line varied between -97km/s÷-16km/s, 0.09Å÷0.37Å and 2km/s÷118km/s, 0.02Å÷0.48Å, respectively. But the radial velocity and the equivalent width of the H_β line vary within -44 km/s÷-4km/s and 1.03Å÷1.31Å.

As can be seen the spectral parameters and the profiles of the H_β line were found to change significantly. Figure 1b shows that as an example, the H_β line profiles obtained in 2010 and 2014. It is evident from Table 1 that the equivalent width of H_β increases when H_α disappears. On the other hand, as is evident from Table 1 and Fig.1b, the H_β line is redshifted when there is no H_α profile.

HD187982. Profile of the H_α line is P Cyg type. On the basis of the observed spectra the profiles of the H_α and H_β lines were investigated. The radial velocities and equivalent widths of the studied lines are determined. In the spectra of HD187982 observed on 01.09 and on 06.09.2014 the profiles of the H_α lines consist of a strong absorption component and a weak emission component which is observed on the red wing of the H_α line (Fig. 2a). It is also interesting that from emission component of the H_α line to longer wavelength there is a weak absorption component again. But in the spectra of 02.10.2013 and 03.10.2013 the H_α line is visible only in absorption and there are no accompanying components.

Apparently from Fig. 2b, in all cases, in the profiles of the H_β line structural changes aren't observed. If we follow the radial velocities of H_α and H_β lines, we will see that the radial velocity of H_α line changes.

It was revealed that change of the radial velocity in the H_β line shows interesting similarity to the form of H_α profile. As it was underlined above, in the spectra of HD187982 star the profile of the H_α line is observed in two following forms:

I. the profile of the H_α line consists of a strong absorption component and a weak emission component which is observed on the red wing of the H_α line.

II. the profile of the H_α line is observed in pure absorption.

On 01.09.2013, 06.09.2013, 02.10.2013 and 03.10.2013 dates in the spectra of HD187982 star the radial velocity of the H_β line there were -33 km/s, -33 km/s, -18 km/s and -19 km/s, respectively.

Table 2 presents some measurements in the H_α and H_β lines in the spectra of HD187982 star obtained in 2010 and 2014.

Apparently, upon transition of the H_α profile from I to II form, the H_β line moves to the red side, that is, the radial velocity changes sharply, but at the equivalent width of H_β line no significant variability was observed (Table 2). But upon such transition the equivalent width of the H_α increases.

The further spectra of this star are observed between June 21, 2014, and August 09, 2014 dates. In the spectra observed from June 21 to August 09, 2014 dates the radial velocity of H_α and H_β changed on average on ±4 km/s.

Next observations of this star were carried out from May 27, 2015 to September 04, 2015. The radial velocities of H_α and H_β lines changed between -30 km/s÷-14 km/s and -33 km/s÷-5 km/s. Table 2 also shows that the equivalent widths of H_α and H_β lines changed with time significantly in the observation periods. However, we didn't find periodicity in such changes. Therefore we suggest that to reveal periodic processes additional observation materials is necessary.

So, investigations above showed that HD198478 and HD187982 are spectroscopically variable, especially RVs changes differently with time. Therefore we also investigated other numerous spectral lines in the considered spectra. We estimated the radial velocities of the strong and basically weak absorption lines formed in deeper layers of atmosphere. All measurements were presented in the Table 3 and Table 4. We averaged the values of velocities of all photospheric absorption lines and determined for mean velocities, $V_r^{\prime}$=-8.5 km/s and $V_r^{\prime\prime}$=-3.0 km/s, respectively. As seen these values are close to the velocities of the mass centers of HD198478 and HD187982 stars (V_r=-7.2 km/s and V_r=-2.9 km/s) which are presented in SIMBAD Astronomical Database.

On the other hand we constructed dependences of radial velocities on residual intensities $V_r(r)$ for these lines (Fig.3). If the dependence of V_r on r exists, it can be considered as "kinematic slice" of the atmosphere. Fig.3 shows that approximately from r=0.75 to r→1 and from r=0.55 to r→1, these changes are almost close to the horizontal straight line with a sharp break. Such forms of the curves $V_r(r)$ are characteristic of the majority of the B and A supergiants.

III. RESULTS AND DISCUSSION

The analysis of the emission and absorption components of the H_α lines showed that the radial velocities change rapidly with time. These changes may be a sign of complex motions in the atmosphere of the star HD198478. Observations showed that H_α disappears on July 02-04, 2010 and on September 07, 2014 (Fig.1a).

A possible explanation is that when the stellar wind matter is moving away from the observer, the central frequencies of the emission and absorption components can be the same and compensate for each other, which may lead to the disappearance of the H_α profiles. The H_β line is known to form in deeper atmospheric layers than H_α. It follows from Table 2 that, on July 02-04, 2010, and on September 07, 2014, the H_β line was shifted to longer wavelengths. These observational facts could be an argument for the possible movement of stellar wind matter away from the observer up to the H_β line formation layers at the time of the disappearance of the H_α lines.

The discovered observational evidence suggests that the non-stationary atmosphere of the star HD198478 may partly be due to the non-spherical stellar wind [17-19].

The profile of the H_α line observed in the atmosphere of the HD187982 supergiant indicates also variable structure. The radial velocities of the H_α and H_β lines change with time.

As seen from Fig.2a the absorption in the line of H_α has variable structure in the spectrum of the star HD187982 depending on the activity phase of the atmosphere. The profile of the line has normal P Cyg type in the active phase of the star atmosphere. The emission component in the red wing of the profile forms and disappears. It is supposed that such variations may be due to non-stationary and strong flow substance in the atmosphere of this star. The radial velocity and spectral parameters of H_β line changes with time too.

We can see from Table 3 and Table 4 on June 19, 2014, and on October 03, 2013, the radial velocities of lines H_α and H_β lines which they are -82 km/s, -38 km/s and -16 km/s, -18.6 km/s, respectively. But the average velocities of the most photospheric absorption lines are approximately same with the velocities of mass centers (See Fig.3). From these observational facts we can also conclude about the dynamical stability of the very deeper layers in which photospheric absorption lines are formed.

As seen the radial velocities of only H_α and H_β lines differ sharply from the velocity of the mass center of the star HD198478 (~73 km/s and ~29 km/s). But for HD187982 those changes are ~13 km/s and ~16 km/s.

So, we can conclude that at that time there is an increasing rate of movement to the upper layers of the atmosphere i.e. there is outflow of matter from the star HD198478. In this case, especially the upper layers of the atmosphere of the star HD198478 is expanding. These observational facts suggest that at this phase the atmosphere of the star has an activity.

The upper layers of the atmosphere of HD187982 star is also expansion phase, but the velocity of expansion is very slow than HD198478 star.

It is known that the H_α and H_β lines form in the upper layers of the stellar atmosphere, in the region of generation of stellar wind [20]. The variable wind and its accelerated motion in supergiants is caused by the strong flux of radiation from the star. Outer atmospheres of supergiant stars are exposed to more intense changes than internal.

Thus, the stellar radiation flux and the variable stellar wind lead to corresponding changes in the outer layers of the atmosphere and the star envelope. As a result, we observe variable absorption and emission components of different forms of the H_α line P Cyg-profile of the star.

On the other hand as is known, the variable stellar wind in the supergiants is caused by the pulsation [21]. If these changes in the stars HD198478 and HD187982 are associated with the pulsation, they should occur periodically. But the amount of obtained data and their inconsistency in observation time does not make it possible to make such far-reaching conclusions in this paper.

For detailed investigation of these events, additional systematic observations of these stars with high resolution are planned at the Shamakhy Astrophysical Observatory in the near future.

IV. CONCLUSION

1. The H_α profile of the hydrogen presented a complicated structure and a time variation for HD198478 star.

First time a P Cyg type profile of the H_α line has been found to occasionally disappear in the spectra of this supergiant star in 2010. This behavior has repeated in 2014 again.

This event may be a manifestation of a non-stationary atmosphere of the star or a non-spherical stellar wind. It is the result of the interaction of the variable stellar wind with the flux of material directed away from the observer. This time the emission line is compensated by the shifted toward the red side absorption line in the H_α profile.

2. When the H_α line disappears or becomes faint the H_β line is displaced to the relatively longer wavelengths.

3. It has been revealed that absorption in the line of H_α has variable structure in the spectrum of the star HD187982 depending on the activity phase of the atmosphere. The profile of the line has normal P Cyg type in the active phase of the star atmosphere. The emission component in the red wing of the profile forms and disappears. It is supposed that such variations may be due to non-stationary and strong flow substance in the atmosphere of this star.

REFERENCE

1. M.J.Barlow, M.Cohen, Infrared photometry and mass loss rates for OBA supergiants and of stars, *Astrophysical Journal*, 1977: 213: 737-755.
2. N.Markova and J.Puls, Bright OB stars in the Galaxy. IV. Stellar and wind parameters of early to late B supergiants, *Astronomy and Astrophysics*, 2008: 478: 823-842.
3. D.R. Gies and D.L.Lambert, Carbon, Nitrogen and Oxygen abundances in early B-type stars, *Astrophysical Journal*, 1992: 387: 673-700.
4. E.Verdugo, A.Talavera, and A.I.Gomez de Castro, Understanding A-type supergiants: II. Atmospheric parameters and rotational velocities of Galactic A-type supergiants, *Astronomy & Astrophysics*, 1999: 346: 819-830.
5. E.Verdugo, A. Talavera, and A.I.Gomez de Castro, Understanding A-type supergiants: Ultraviolet and visible spectral atlas of A-type supergiants, *Astronomy & Astrophysics*, 1999: 137: 351-362.
6. C.J.Evans and Ian D. Howarth , Characteristics and classification of A-type supergiants in the Small Magellanic Cloud, *MNRAS*, 2003: 345: 1223-1235.
7. N.Przybilla, M.Firnstein, M.F.Nieva, G.Meynet, and A.Maeder, Mixing of CNO-cycled matter in massive stars, *Astronomy and Astrophysics*, 2010: 517: 1-6.
8. P.A.Crowther, D.J. Lennon and N.R.Walborn, Physical parameters and wind properties of galactic early B supergiants, *Astronomy and Astrophysics*, 2006: 446: 279-293.
9. A.B.Underhill, Some observations of the supergiants 67 Ophiuchi, 55 Cygni, and χ^2 Orionis, *Dominion Astrophysical Observatory Victoria*, 1960; 11(18): 353-361.
10. P.Granes, Evolution du spectre de la supergeante 55 Cygni, *Astronomy & Astrophysics*, 1975 : 45 : 343-347.
11. H.A.Abt and N.I.Morrell, The relation between rotational velocitites and spectral peculiarities among A-type stars, *The Astrophys.J., Suppl. Ser.*1995: 99: 135-172.
12. R.L.Snell and P.A.Vanden Bout, High-resolution profiles of the 5780Å interstellar diffuse Band, The Astrophys.J., 1981: 244: 844-847.
13. Kh.M.Mikailov, V.M.Khalilov, and I.A.Alekberov, Echelle-spectrometer of Kassegren focus of the two-meter telescope of the Shamakhy Astrophysical Observatory, *Tsirk. ShAO*, 2005: 109: 21-29.
14. G.A.Galazutdinov, *Prepr. SAO RAS*, *92(2);* 1992 .
15. L.H.Aller, Atmospheres of the B stars. II. The supergiant 55 Cygni, *American Astronomical Society*, 1956: 133-138.
16. Y.M.Maharramov, Spectral variability of the star 55 Cyg B3Ia, *Astronomy Reports*, 2013; 57(4): 303-309.
17. J.D.Rosendhal, Survey of H-alpha emission in early-type high-luminosity stars, *Astrophys.J.* 1973: 186: 909-937.
18. V.V.Sobolev, *Moving Envelopes of Stars,* (Nauka, Moscow; 1947; Harvard Univ., Press, Harvard; 1960).
19. V.V.Sobolev, *Course in Theoretical Astrophysics Sci.* (Nauka, Moscow; 1967; NASA, Washington, DC; 1969).
20. C.de Jager, *The Brightest Star*, (Reidel, Dordrecht; 1980; Mir, Moscow; 1984)
21. J.P.Cox, *Theory of Stellar Pulsation* (Princeton Univ. Press, Princeton; 1980; Mir, Moscow; 1983).

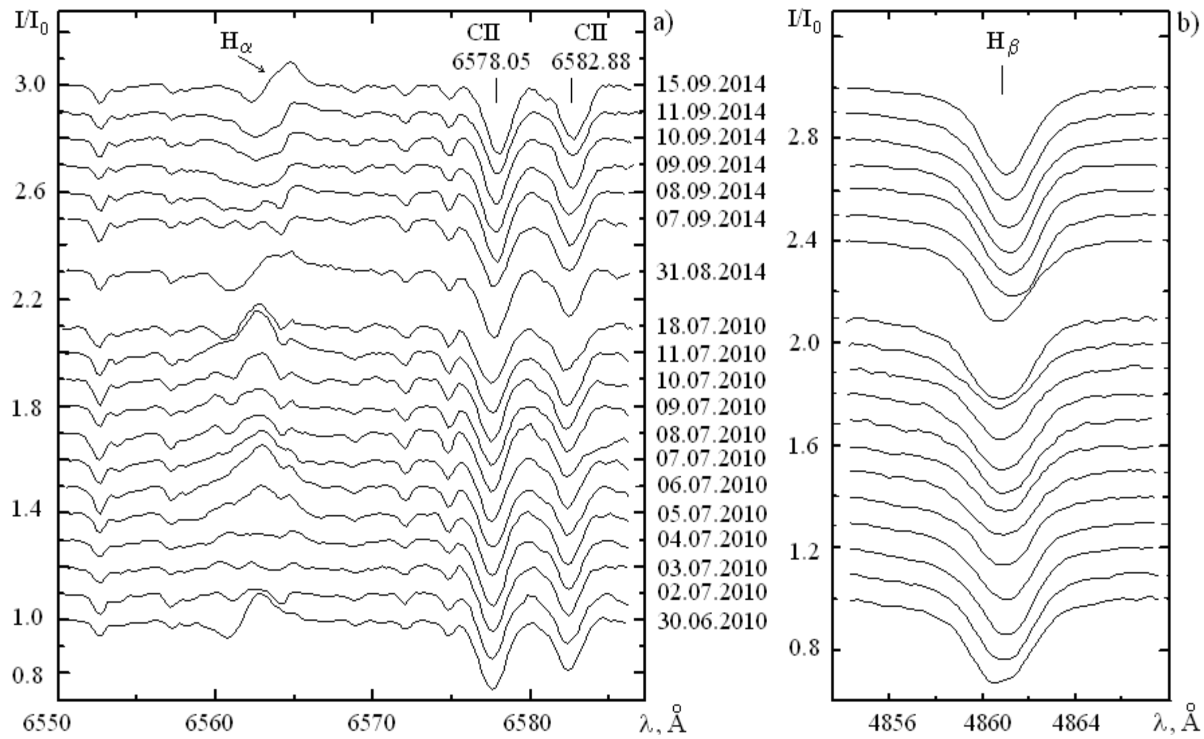

Figure 1. Profiles of the H_α and H_β lines in the spectra of HD187982 observed in 2010 and 2014.

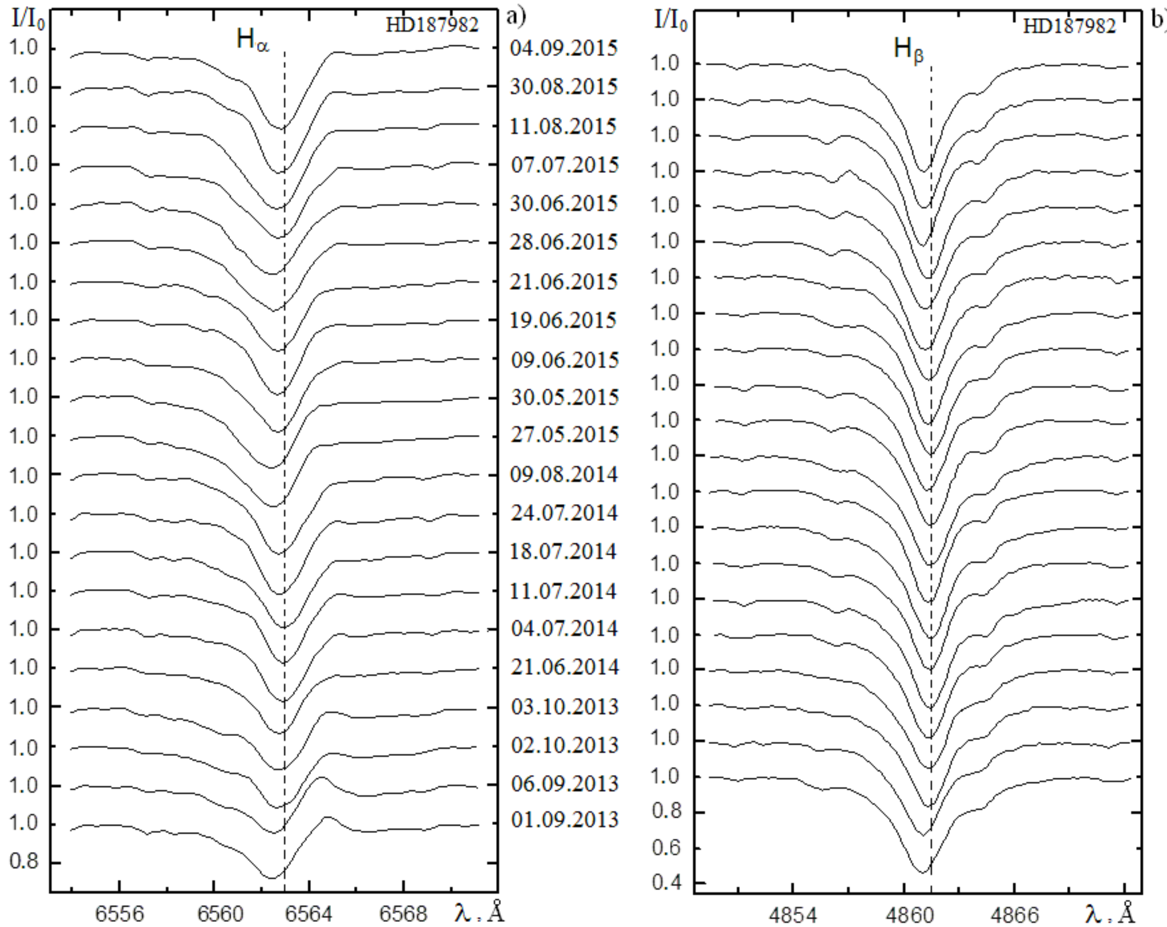

Figure 2. Profiles of the H_α and H_β lines in the spectra of the star HD187982 observed in 2013-2015.

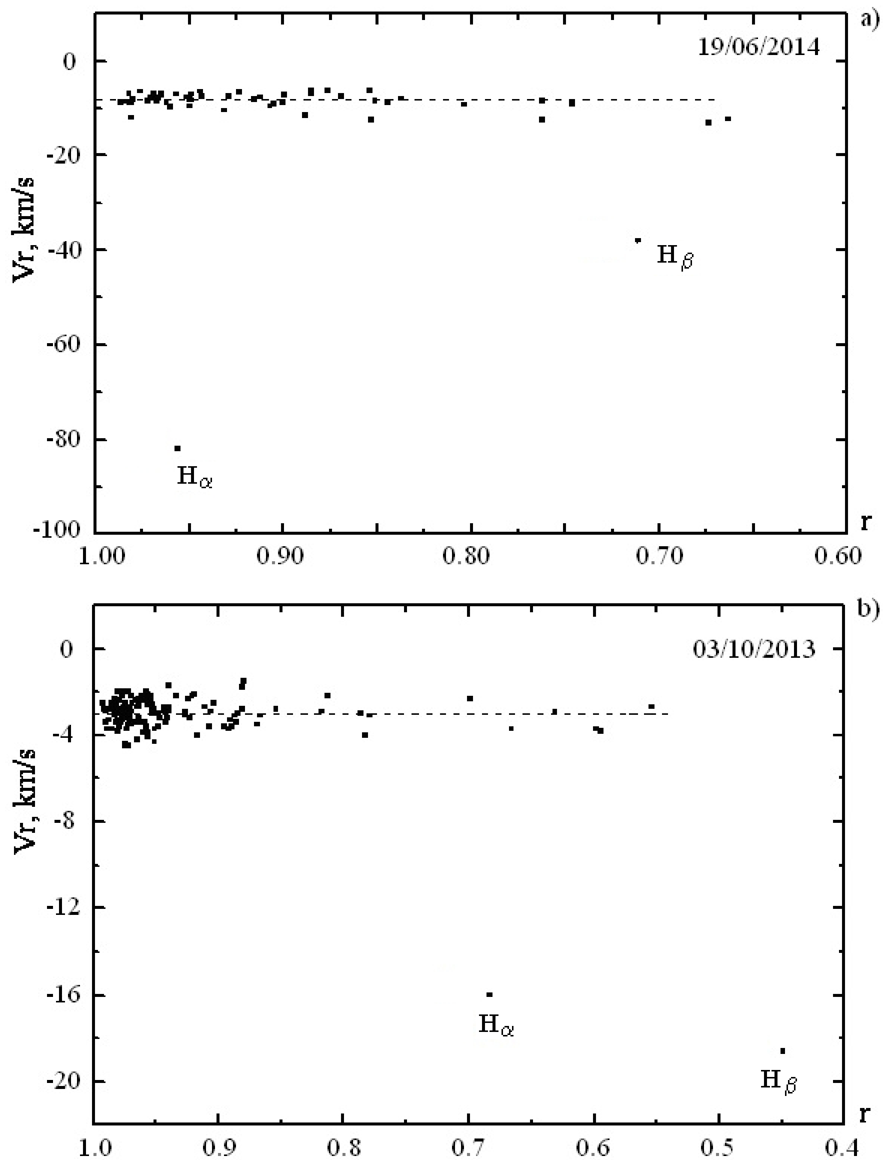

Figure 3. Kinematic slices: a) for HD198478 and b) for HD187982

Table 1. Measurement of the radial velocities and equivalent widths.

HD198478 Date, JD	Vr(abs) km/s H_α	W (abs) Å H_α	Vr(em) km/s H_α	W(em) Å H_α	Vr(abs) km/s H_β	W (abs) Å H_β
2455378.30	-97	0.17	23	0.22	-22	1.27
2455380.34	?	?	?	?	-15	1.31
2455381.38	?	?	?	?	-13	1.31
2455382.33	?	?	?	?	-14	1.17
2455383.30	-	-	13	0.32	-20	1.04
2455384.33	-	-	23	0.46	-23	1.03
2455385.38	-	-	5	0.34	-20	1.10
2455386.37	-	-	2	0.12	-16	1.17
2455387.37	-	-	3	0.18	-17	1.18
2455388.33	-	-	6	0.23	-23	1.06
2455389.33	-	-	6	0.48	-29	1.04
2455396.32	-90	0.07	6	0.14	-29	1.22
2456901.22	-89	0.15	88	0.20	-44	1.09
2456908.21	?	?	?	?	-4	1.30
2456909.26	-30	0.29	-	-	-13	1.05
2456910.16	-21	0.37	106	0.02	-14	1.16
2456911.10	-16	0.23	94	0.03	-17	1.19
2456912.13	-21	0.27	118	0.06	-19	1.14
2456916.26	-29	0.09	84	0.15	-21	1.09

Table 2. Measurement of the radial velocities and spectral parameters.

HD187982 Date, JD	Vr(abs) km/s H_α	W(abs) Å H_α	Vr(em) km/s H_α	W(em) Å H_α	Vr(abs) km/s H_β	W(abs) Å H_β
2456537.21	-29	0.89	79	0.20	-33	2.46
2456542.20	-23	0.77	70	0.30	-33	2.26
2456568.21	-18	1.29	-	-	-18	2.40
2456569.23	-17	1.33	-	-	-19	2.42
2456830.36	-11	1.06	-	-	-16	2.35
2456843.34	-5	1.15	-	-	-9	2.53
2456850.29	-6	1.10	-	-	-13	2.41
2456857.38	-5	1.33	-	-	-8	2.57
2456863.30	-12	1.36	-	-	-14	2.41
2456879.29	-13	1.38	-	-	-12	2.80
2457170.36	-24	1.30	-	-	-6	2.31
2457173.35	-30	1.29	-	-	-14	2.28
2457183.47	-17	1.23	-	-	-5	2.20
2457193.45	-19	1.15	-	-	-15	2.42
2457195.43	-16	1.22	-	-	-14	2.34
2457202.36	-25	1.29	-	-	-23	2.45
2457204.31	-27	1.36	-	-	-25	2.31
2457211.34	-16	1.48	-	-	-18	2.13
2457246.29	-19	1.59	-	-	-33	1.98
2457265.40	-14	1.39	-	-	-30	2.23
2457270.39	-14	1.70	-	-	-30	2.23

Table 3. The identification of lines, residual intensities (r) and heliocentric radial velocities (Vr) in spectra HD198478.

19.06.2014					
Elements, λ, Å	Vr, km/s	r_v	Elements, λ, Å	Vr, km/s	r_v
CII 6582.88	-9.2	0.804	SII 5606.15	-8	0.966
CII 6578.05	-9	0.746	NII 5495.67	-7.1	0.957
H_α 6562.816	-82	0.956	SII 5473.62	-6.8	0.969
NeI 6506.53	-7	0.965	SII 5453.83	-8.7	0.900
NII 6482.05	-7.7	0.912	SII 5432.82	-10.5	0.931
NeI 6402.25	-7.5	0.929	SII 5428.67	-9.6	0.960
NeI 6382.99	-12	0.981	SII 5345.72	-7.9	0.969
SiII 6371.36	-8.2	0.915	SII 5320.73	-7.4	0.965
SiII 6347.10	-11.5	0.888	FeII 5316.65	-8.8	0.982
SiII 6312.66	-8.8	0.981	FeIII 5193.89	-7.7	0.970
NeI 6163.59	-8.6	0.984	FeII 5169.03	-7.1	0.949
NeI 6143.06	-9.5	0.950	OII 5160.02	-8.8	0.986
NeI 6074.34	-8.7	0.981	FeIII 5156.12	-6.7	0.923
HeI 5875.72	-13	0.674	CII 5145.16	-8.7	0.962
NaI D1	-11.6	0.356	CII 5133.12	-6.5	0.976
NaI D2	-10.6	0.408	HeI 5047.74	-12.4	0.853
FeIII 5833.93	-6.4	0.944	NII 5045.10	-6.3	0.876
NII 5747.30	-8.5	0.967	SII 5027.22	-8.2	0.980
SiIII 5739.73	-6.2	0.854	FeII 5018.44	-8.3	0.949
AlIII 5722.73	-9	0.905	HeI 5015.68	-12.6	0.762
NII 5710.77	-7.3	0.899	NII 5007.33	-7.5	0.943
AlIII 5696.60	-8.5	0.851	NII 5005.15	-6.2	0.885
NII 5686.21	-7	0.885	NII 5001.4	-8.8	0.844
NII 5679.56	-8.4	0.762	SII 4994.36	-7.7	0.951
NII 5676.02	-7.5	0.869	SII 4991.97	-6.9	0.982
NII 5666.63	-8	0.837	OII 4941.12	-8.3	0.980
SII 5659.99	-8.4	0.972	HeI 4921.93	-12.3	0.663
SII 5647.03	-8.2	0.950	SII 4917.21	-7.9	0.968
SII 5639.97	-9.5	0.907	H_β 4861.337	-38	0.711

Table 4. The identification of lines, residual intensities (r) and heliocentric radial velocities (Vr) in spectra HD187982.

03.10.2013					
Elements, λ, Å	Vr, km/s	r_v	Elements, λ, Å	Vr, km/s	r_v
H_α 6562.816	-16	0.683	SII 5432.82	-2.7	0.940
NeI 6506.53	-7.4	0.970	FeII 5425.25	-2.9	0.926
FeII6456.38	-3.0	0.786	CrII 5420.93	-2.9	0.981
FeII 6446.41	-3.4	0.968	CrII 5407.62	-3.3	0.980
FeII 6432.68	-1.7	0.940	FeII 5395.96	-2.9	0.973
FeII 6416.93	-2.1	0.919	FeII 5393.85	-2.7	0.984
NeI 6402.25	-3.2	0.977	FeII 5387.07	-2.8	0.952
SiII 6371.36	-2.9	0.631	FeII 5375.84	-3.3	0.981
SiII 6347.10	-2.7	0.554	FeII 5370.30	-3.0	0.978
FeII 6331.96	-2.2	0.954	FeII 5362.87	-2.9	0.818
FeII 6317.99	-2.2	0.934	FeII 5339.59	-2.0	0.958
AlII 6243.37	-2.2	0.970	FeII 5337.73	-3.1	0.973
FeII 6238.39	-2.5	0.904	FeII 5325.56	-2.1	0.919
FeII 6175.16	-3.9	0.956	FeII 5316.66	-3.7	0.666
OI 6158.18	-12.0	0.925	CrII 5313.58	-3.2	0.941
OI 6156.77	-17.0	0.932	CrII 5310.69	-2.9	0.983
FeII 6149.25	-4.0	0.917	CrII 5308.42	-3.3	0.971
FeII 6147.74	-2.7	0.911	CrII 5305.86	-2.6	0.957
FeII 6103.54	-4.4	0.974	MnII 5302.32	-2.8	0.980
FeII 6084.10	-2.0	0.972	FeII 5291.67	-3.0	0.953
PII 6043.12	-2.4	0.960	FeII 5284.10	-2.2	0.921
FeII 5991.37	-2.2	0.961	CrII 5279.86	-2.6	0.974
SiII 5978.93	-1.8	0.881	FeII 5276.00	-2.8	0.854
FeII 5961.71	-2.6	0.953	FeII 5272.39	-2.1	0.956
SiII 5957.56	-2.8	0.881	FeII 5264.80	-3.4	0.886
NaI 5895.92	-2.5	0.565	FeII 5260.26	-3.7	0.892
NaI 5889.95	-3.8	0.523	FeII 5257.11	-2.4	0.966
HeI 5875.72	-1.5	0.880	FeII 5254.93	-3.1	0.926
SiII 5868.40	-2.5	0.992	FeII 5251.24	-2.9	0.943
FeII 5835.49	-3.3	0.987	CrII 5249.43	-2.3	0.983
FeII 5813.67	-3.2	0.974	CrII 5237.32	-2.9	0.906
FeII 5726.56	-2.9	0.979	FeII 5234.62	-4.0	0.783
SII 5606.15	-2.0	0.977	FeII 5227.49	-3.3	0.891
FeII 5588.21	-3.5	0.970	FeII 5216.85	-2.7	0.943
FeII 5577.92	-4.5	0.975	CrII 5210.85	-3.7	0.985
FeII 5544.76	-4.3	0.951	CrI 5206.04	-2.8	0.988
FeII 5534.84	-3.1	0.867	FeII 5203.64	-2.0	0.981
FeII 5510.78	-2.2	0.977	FeII 5197.58	-3.1	0.779
CrII 5508.62	-2.7	0.976	TiII 5188.69	-3.7	0.951
FeII 5506.20	-3.2	0.923	SiII 5185.54	-2.5	0.969
FeII 5503.22	-3.6	0.958	MgI 5183.61	-3.6	0.907
FeII 5487.63	-3.6	0.948	FeII 5180.32	-3.1	0.983
FeII 5482.32	-2.5	0.963	FeII 5177.39	-2.9	0.970
CrII 5478.37	-3.9	0.960	MgI 5172.69	-3.0	0.948
FeII 5466.92	-3.4	0.942	FeII 5169.03	-2.3	0.699
SII 5453.83	-3.0	0.976	FeII 5149.46	-2.8	0.953

Table 4. Continue.

03.10.2013					
Elements, λ, Å	Vr, km/s	r_v	Elements, λ, Å	Vr, km/s	r_v
FeII 5146.12	-2.7	0.965	HeI 5015.68	-2.8	0.971
FeII 5144.36	-3.2	0.963	SII 5009.56	-4.5	0.972
FeII 5136.80	-3.0	0.978	FeII 5007.45	-3.1	0.971
FeII 5132.67	-2.8	0.977	FeII 5004.20	-2.3	0.924
FeII 5127.86	-2.4	0.957	FeII 5001.92	-3.6	0.895
FeII 5120.34	-2.8	0.991	FeII 4993.35	-3.2	0.947
FeII 5117.03	-2.8	0.988	FeII 4990.50	-2.4	0.955
FeII 5106.11	-2.5	0.985	FeII 4984.50	-2.3	0.964
FeII 5100.74	-3.6	0.889	FeII 4977.03	-2.7	0.971
FeII 5097.27	-3.9	0.957	FeII 4969.36	-3.3	0.977
FeII 5093.57	-2.3	0.954	FeI 4957.59	-3.4	0.978
FeII 5089.22	-3.0	0.976	FeII 4951.59	-2.4	0.956
FeII 5087.26	-2.4	0.979	FeII 4948.10	-2.6	0.981
FeII 5082.23	-2.8	0.981	FeII 4923.92	-8.3	0.595
FeII 5075.77	-2.7	0.964	SII 4917.21	-3.4	0.982
FeII 5074.05	-3.0	0.975	FeII 4913.30	-3.7	0.973
TiII 5072.30	-2.9	0.990	TiII 4911.19	-3.8	0.980
FeII 5070.90	-3.5	0.972	FeII 4908.15	-3.4	0.990
FeII 5061.72	-2.5	0.974	FeII 4893.81	-2.2	0.977
SiII 5056.06	-3.0	0.884	CrII 4876.40	-3.1	0.887
FeII 5047.64	-2.6	0.956	H_β 4861.34	-18.6	0.449
FeII 5045.11	-2.7	0.983	CrII 4848.25	-3.0	0.885
SiII 5041.03	-2.2	0.813	CrII 4836.24	-3.4	0.963
FeII 5035.71	-2.9	0.940	CrII 4824.14	-3.5	0.869
FeII 5032.71	-4.1	0.956	SII 4815.55	-3.6	0.979
FeII 5022.79	-3.4	0.959	TiII 4779.98	-4.2	0.965
FeII 5018.44	-5.7	0.598	MnII 4764.70	-3.7	0.989